第 34 卷 第 3 期 原 子 核 物 理 评 论 Vol. 34, No. 3
2017 年 9 月 Nuclear Physics Review Sep., 2017

Article ID: 1007-4627(2017) 03-0481-07

Possible Properties on Nuclear Shape and Stiffness Evolution: A Systematic Analysis Based on Nuclear-Energy-Surface Calculations

MENG Haiyan[1], WANG Hualei[1,†], CHAI Qingzhen[1], ZHANG Sha[1], YANG Jie[1], LIU Minliang[2]

(*1. School of Physics and Engineering, Zhengzhou University, Zhengzhou 450001, China;*
2. Institute of Modern Physics, Chinese Academy of Sciences, Lanzhou 730000, China)

Abstract: Nuclear shape and stiffness evolutions in even-even nuclei with $50 < Z < 82$ are systematically analyzed in terms of the pairing-deformation self-consistent nuclear-energy-surface calculation in $(\beta_2, \gamma, \beta_4)$ deformation space. Calculated equilibrium deformations are presented and compared with other theoretical predictions and available experimental data. The stiffness parameters C_β and C_γ respectively related to quadrupole deformations β_2 and γ are determined from the deformation energy curves, which are consistent with the observed low-lying β and/or γ bands. The stiffness evolution under rotation along the yrast line is briefly discussed, *e.g.*, on the basis of the centipidelike E-GOS curves, showing an unnegligible vibration effect.

Key words: nuclear shape; stiffness parameter; nuclear-energy-surface calculation
CLC number: O571.42 **Document code:** A **DOI:** 10.11804/NuclPhysRev.34.03.481

http://www.npr.ac.cn

1 Introduction

As is well known, nuclear shape arises from basic correlations in a nucleus[1]. The study on nuclear shape and their evolution with different degrees of freedom (*e.g.*, nucleon number, angular momentum and excitation energy) is important to reveal and understand these correlations. Due to them, different intrinsic shapes may appear in different nuclear configurations. Moreover, much work has been done both theoretically and experimentally to reveal the symmetry breaking mechanism and to obtain conclusive evidence[2]. Sometimes, it is found that the situations are rather complicated, especially in transition nuclei where the nuclear wave function may be a superposition of states corresponding to different shapes. At this time, the potential-energy surface is normally very flat over a large deformation domain and the so-called equilibrium deformations identified from the minimum of such a flat surface will be practically meaningless since they may be strongly affected by the model parameters. However, the shape stiffness related to the flatness of the energy landscape is relatively model independent, which can be used to describe the nuclear properties to some extent.

In our previous work[3–9], the shape stiffness evolutions are respectively investigated in different isotopes. Partly based on these results, we will try to systematically analyze the possible properties on nuclear shape and stiffness evolution in the nuclear region with $50 < Z < 82$ where the present model parameters are generally considered to be more valid. This paper is organized as follows. After the introduction, we will briefly outline the unified calculation method and simultaneously provide the necessary references in Sec. 2. The numerical results and discussion are presented in Sec. 3. Then, a summary is given in Sec. 4.

2 Model

The nuclear-energy-surface(NES) calculation usually accounts well for the overall systematics of nuclear shape and stiffness, especially in medium and heavy mass nuclei. Strictly speaking, the NES calculation includes the potential-energy-surface

Received date: 30 Oct. 2016; **Revised date:** 19 Apr. 2017
Foundation item: National Natural Science Foundation of China(11675148); Outstanding Young Talent Research Fund of Zhengzhou University (1521317002); Physics Research and Development Program of Zhengzhou University (32410017); Foundation and Advanced Technology Research Program of Henan Province (162300410222)
Biography: MENG Haiyan(1992–), female, Hengshui, Hebei, Master, working on nuclear physics;
† **Corresponding author:** WANG Hualei, Email: wanghualei@zzu.edu.cn.

(PES) calculation[10] and total-routhian-surface (TRS) calculation[11, 12]. Nowadays, as one of the most powerful theoretical tools in the study of nuclear structure, the NES approach has several standard components, each one individually familiar from the literature. Here, we will briefly outline the unified procedure and simultaneously provide the necessary references. In the PES calculation which is based on macroscopic-microscopic model[10], the total potential energy calculated as a function of shape, proton number Z, and neutron number N is the sum of a macroscopic term and a microscopic term representing the shell correction[10, 13]. The macroscopic term changes smoothly as a function of particle number and deformation. The microscopic term can have rapid fluctuation with changing deformation and particle number. The macroscopic energy is obtained from the standard liquid-drop model[14]. The shell correction energy is calculated by the Strutinsky method[15, 16] with a smoothing range $\gamma = 1.20\hbar\omega_0$ ($\hbar\omega_0 = 41/A^{1/3}$ MeV), and a correction polynomial of order $p = 6$. The single-particle levels is derived from the deformed Woods-Saxon(WS) potential with the set of universal parameters[17]. These WS parameters, taken from Ref. [18], are:

(a) Radius parameters:
$r_0(\mathrm{p}) = 1.275$ fm, $r_0(\mathrm{n}) = 1.347$ fm,
$r_{0-\mathrm{so}}(\mathrm{p}) = 1.320$ fm, $r_{0-\mathrm{so}}(\mathrm{n}) = 1.310$ fm.
(b) Central potential depth parameters:
$V_0 = 49.6$ MeV, $\kappa = 0.86$.
(c) Spin-orbit potential strength constants:
$\lambda(\mathrm{p}) = 36.0$, $\lambda(\mathrm{n}) = 35.0$.
(d) Diffuseness parameters:
$a_0(\mathrm{p}) = a_0(\mathrm{n}) = 0.70$ fm,
$a_{0-\mathrm{so}}(\mathrm{p}) = a_{0-\mathrm{so}}(\mathrm{n}) = 0.70$ fm.

The pairing correlation is treated using the Lipkin-Nogami (LN) approach[12, 19] in which the particle number is conserved approximately and thus the spurious pairing phase transition encountered in the usual BCS calculation can be avoided. The pairing-deformation self-consistent PES can be obtained in a selected deformation space, *e.g.*, in (β_2, γ, β_4). Based on the PES, the nuclear equilibrium deformation and stiffness may be determined. Under rotation, the TRS calculation will be adopted where the cranking term is taken into account (For more details, see, Ref. [3] and references therein). Note that, in the TRS calculation, a set of cranking WS parameters[20] is usually used, which is:

(a) Radius parameters:
$r_0(\mathrm{p}) = r_0(\mathrm{n}) = 1.190$ fm,
$r_{0-\mathrm{so}}(\mathrm{p}) = r_{0-\mathrm{so}}(\mathrm{n}) = 1.190$ fm.
(b) Central potential depth parameters:
$V_0 = 53.754$ MeV, $\kappa = 0.791$.
(c) Spin-orbit potential strength constants:
$\lambda(\mathrm{p}) = \lambda(\mathrm{n}) = 29.494$.
(d) Diffuseness parameters:
$a_0(\mathrm{p}) = a_0(\mathrm{n}) = 0.637$ fm,
$a_{0-\mathrm{so}}(\mathrm{p}) = a_{0-\mathrm{so}}(\mathrm{n}) = 0.637$ fm.

Such a parameter set, which is quite successful in accurately reproducing energies of single-particle as well as collective states, can give a better description for charge radii (both magnitude and isospin dependence) and high-spin properties (*e.g.*, moment of inertia) in nuclei (see Refs. [20, 21] and references cited therein), especially in medium and heavy mass regions as discussed below.

3 Results and discussion

In this investigation, we will focus on two isotopic chains, namely, Ba and Os ones, which are respectively close to proton magic numbers 50 and 82. In nuclear structure research, some phenomenological quantities, such as the energy ratio $R_{4/2}$ ($R_{4/2} \equiv E_{4_1^+}/E_{2_1^+}$) and the P-factor ($P \equiv N_\mathrm{p}N_\mathrm{n}/(N_\mathrm{p}+N_\mathrm{n})$)[22–26], are usually used to evaluate the nuclear collectivities. Figure 1 shows the contour maps of the available phenomenological ratio $R_{4/2}$ and the P factor for even-even nuclei with $50 \leqslant Z \leqslant 82$. The energy ratio $R_{4/2}$ is 3.3 for a well-deformed axially symmetric rotor, about 2.9 for the critical point of deformed to spherical path, 2.5 for γ-unstable vibrator, 2.2 for the critical point of γ-unstable vibrator to spherical path and 2.0 for spherical vibrator, which respectively correspond to $SU(3)$, $X(5)$, $O(6)$, $E(5)$ and $U(5)$ dynamic symmetries in the algebraic view of the interacting boson model (IBM)[27–29]. Nuclear deformation may be explained as due to a competition between the pairing interaction of like nucleons and the neutron-proton interaction which is responsible for strong mixing of shell model configurations. The P-factor can just be viewed as the average number of interactions of each valence nucleon with those of the other type. Casten *et al.*[22] have pointed out that the transition to deformation generally occurs when $P \approx 4-5$, that is, each valence nucleon interacts with about 4–5 nucleons of the other type. Of course, it should be related to the relative integrated strengths of the p−n and like-nucleon-pairing interactions. The global property in this region can be seen from Fig. 1. As expected, the $R_{4/2}$ ratio and P-factor reach the maximum value near the double-midshell nucleus, *e.g.* in ^{170}Dy, indicating the maximum collectivity (the rotational excitation will be favored at this time). They have the decreasing trend

http://www.npr.ac.cn

as the nucleon number moves away from the midshell. Then the deformation will generally decrease and the vibration and single-particle motions may appear.

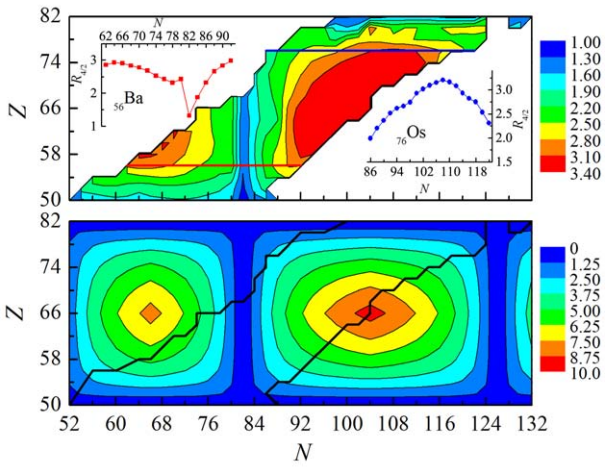

Fig. 1 (color online) The available phenomenological ratio $R_{4/2}$ (upper panel) and the P factor (lower panel) for even-even nuclei between $Z = 50$ and 82 magic proton numbers. As seen in the upper panel, the available $R_{4/2}$ values for Ba (red symbols and line) and Os (blue symbols and line) isotopes are shown as insets. In the lower panel, the boundary lines same to those in the upper panel are plotted.

Fig. 2 shows the calculated ground-state deformations β_2 for even-even Ba and Os isotopes, together with available experiments and the theoretical results based on the fold-Yukawa (FY) single-particle potential and the finite-range droplet model (FRDM)[30] for comparison. Note that the experimental β_2 are deduced from the intrinsic quadrupole moment related to the reduced electric quadrupole transition probability $B(\mathrm{E2})$[31]. As is seen in Fig. 2, the predicted ground state β_2 deformations basically are in agreement with the experimentally measured results though there is still a systematic underestimation for β_2. This agrees with the analysis by Dudek *et al.*[32] where a corrected formula is suggested to modify the shape inconsistency. In addition, as mentioned above, the β_2 deformation reaches a maximum near $N = 66$ and/or $N = 104$ midshell nuclei and decreases as the neutron number N moves away from the neutron midshell number. One also can see that the present results can not completely agree with the FY+FRDM calculation especially in the weakly deformed nuclei which usually have soft shapes as mentioned below. However, it seems that our calculation is more reasonable to some extent. Of course, it should be noted that according to the Lund convention[33], the negative β_2 value just indicates the minimum of the PES has the γ value bewteen 30° and 60°. If the energy surface is very soft in the γ direction, the exact value will be meaningless as described in the introduction.

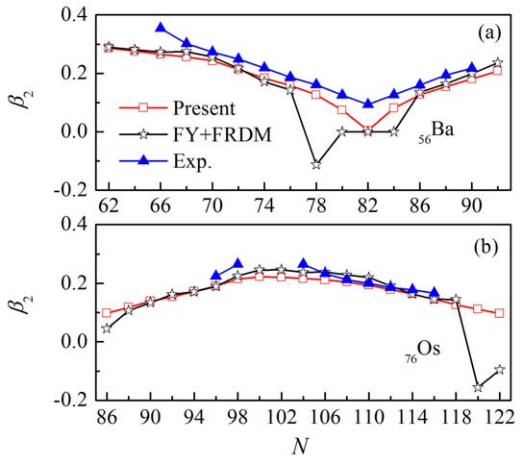

Fig. 2 (color online) Calculated ground-state β_2 deformations for even-even Ba (a) and Os (b) isotopes, compared with the FY+FRDM calculation and partial experimental data.

The equilibrium deformations calculated theoretically may be model-dependent (*e.g.*, see Fig. 2), especially in soft nuclei because these deformations can be strongly affected by Hamiltonian parameters including mean-field and pairing ones. However, the deformation energy curves along different deformation degrees of freedom will usually not depend on the model parameters too much. As shown in Fig. 3, the deformation energy curves against β_2 and γ are given for selected ^{132}Ba and ^{180}Os nuclei. It should be noted that in the actual calculations the Cartesian coordinates $X = \beta_2\cos(\gamma + 30°)$ and $Y = \beta_2\sin(\gamma + 30°)$ are used, where the parameters β_2 and γ specify the magnitude of the quadrupole deformation and the

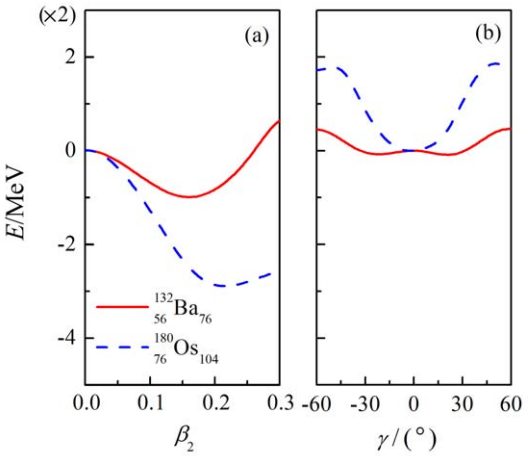

Fig. 3 (color online) Deformation energy curves against β_2 (a) and γ (b) for two selected nuclei ^{132}Ba and ^{180}Os. At each β_2 (γ) point, the energy has been minimized with respect to the γ (β_2) and β_4 deformations.

https://www.npr.ac.cn

asymmetry of the shape, respectively. Thus the β_2 value is positive and the triaxiality parameter covers the range $-120^\circ \leqslant \gamma \leqslant 60^\circ$ according to the Lund convention. For the ground states, in principle, one of the three sectors $[-120^\circ,-60^\circ]$, $[-60^\circ,0^\circ]$ and $[0^\circ,60^\circ]$ is enough to describe the nuclear shape. In Fig. 3, the γ range is shown from -60° to 60° for convenience. Obviously, the corresponding minimum stiffness and depth of one deformation energy curve can be qualitatively evaluated. The stiffnesses may be rather different even for the deformation energy curves with the same equilibrium deformations.

To present a quantitative description for nuclear stiffness, we calculate the corresponding stiffness parameter C_β and C_γ based on a simple harmonic approximation for these two isotopic chains, as shown in Fig. 4. Note that the stiffness constants are determined numerically from the deformation energy curves with respect to the different deformation degrees of freedom. For instance, C_β and C_γ are defined from the following equations[5, 6, 34]:

$$\begin{cases} E = E_{\min} + \dfrac{1}{2} C_\beta (\beta_2 - \beta_2^{\min})^2 \\ E = \dfrac{1}{2} C_\gamma \gamma^2 \end{cases}, \qquad (1)$$

where $E_{\min}$ denotes the the minimum energy and the constants C_β and C_γ can be extracted from the energies at different deformation points (For more details, see Refs. [5, 6, 34]). As shown in Fig. 4, it is found that the calculated stiffness coefficients exhibit irregular oscillating behaviors (Note that the stiffness constant $C_\gamma < 0$ corresponds to a permanently γ deformation, as discussed in Ref. [35]). However, several facts agree well with the experimental observation. For instance, the variation trend of C_β is in good agreement with that of $E_{0_2^+}$ (it is usually suggested to be the bandhead built on the so-called β-vibrations with $K^\pi = 0^+$). The available $E_s/E(2_1^+)$ ratios related to the γ deformation and $E_{2_2^+}$ built on the γ-vibrations with $K^\pi = 2^+$ also have a consistent trend with C_γ[6]. In addition, it is found that nuclear stiffness to a large extent depends on the corresponding proton and/or neutron magic numbers (*e.g.*, the γ or octupole deformation magic numbers) rather than the mass regions.

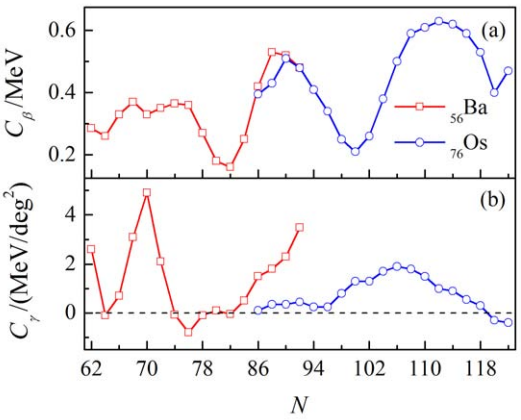

Fig. 4 (color online) Calculated ground-state stiffness parameters C_β (a) and C_γ (b) towards β_2 and γ deformation degrees of freedom, respectively, for even-even Ba (red square symbols) and Os (blue circle symbols) nuclei.

The present TRS approach is a powerful tool in the analysis of high-spin yrast states. However, it does not include the vibration mechanism which usually appears in excited state sequences. It is noticed that there is a rather large difference in moment of inertia between theory and experiment in this region even though the pairing strength is adjusted according to the experimental odd-even difference (*e.g.*, see Refs. [3, 37]), showing the possible appearance of other mechanisms by which atomic nuclei generate angular momentum, such as vibration and single-particle excitations. Indeed, the β and γ vibration phenomena have been systematically observed in this mass region, *e.g.*, in the W[38], Os[39] and Pt[40] isotopes. In order to discern the shape and phase evolution between vibrational and rotational structure in nuclei as a function of spin Regan *et al.*[36] have ever proposed a simple empirical method, called E-GOS (E-Gamma Over Spin) curves. As done by Regan *et al.*[36], the typical E-GOS curves for a perfect harmonic vibrator, γ-soft, and axially symmetric rotors are presented in Fig. 5(a)

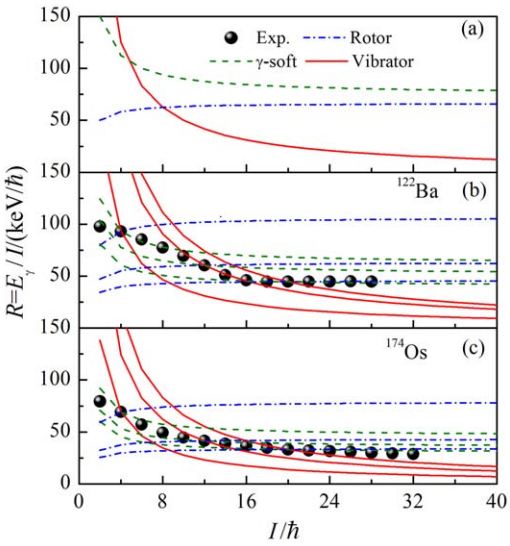

Fig. 5 (color online) (a) The typical E-GOS curves for a perfect harmonic vibrator, γ-soft, and axially symmetric rotors with first 2^+ excitations of 500, 300, and 100 keV, respectively[36]. Similar to (a), three sets of such E-GOS curves at three selected spin pionts $I = 4$, 12 and 20 $\hbar$, together with the experimental data (filled circles) for ^{122}Ba (b) and ^{174}Os (c).

http://www.npr.ac.cn

based on the energy of the first 2^+ state. Further, if we assume that each energy level could be respectively populated by the excitation of a pure vibrator, an idealized γ-soft rotor and an axially symmetric rotor, we can obtain three corresponding E-GOS curves through each spin point, as seen in Fig. 5(b) and (c) (*e.g.*, see Ref. [3, 4] for more details). Moreover, if this assumption of the pure motion mode can be accepted, the corresponding curve will cross some experimental points. From Fig. 5, one actually can see for different spin regions the E-GOS curves with different motion modes may cross several adjacent data points, while none of them can cross all the data, indicating the motion modes change with increasing spins.

Based on this idea mentioned above, in our recent work[3, 4], we developed this traditional method, extending the E-GOS curves to the centipidelike E-GOS curves, which means we just keep the corresponding three curves from $R(I)$ point to its next adjacent point $R(I+2)$. There is no doubt, one can suppose the adjacent data points have the greatest possibility to possess the similar motion modes except for the band-crossing point. There will be (not) a line segment connected the adjacent two points if the motion mode is pure (mixing). It is expected that such improved curves can to an extent more precisely describe the vibrational, γ-soft and rotational evolutions with increasing spins. In Fig. 6, we show such typical centipidelike E-GOS curves for several selected Ba and Os nuclei, indicating the evolutions of the motion modes to a large extent. Obviously, the γ-soft and vibrational properties should be taken into account to a large extent under rotation. Of course, the corresponding stiffness parameters will be affected. It is found that, as expected, the minimum of the corresponding energy curve generally becomes soft when the transition from rotation to vibration occurs while it becomes stiff when the transition from vibration to rotation occurs[3]. In the future, it will be worth investigating the stiffness parameters with non-zero rotational frequencies and the coupling of different motion modes in this region.

http://www.npr.ac.cn

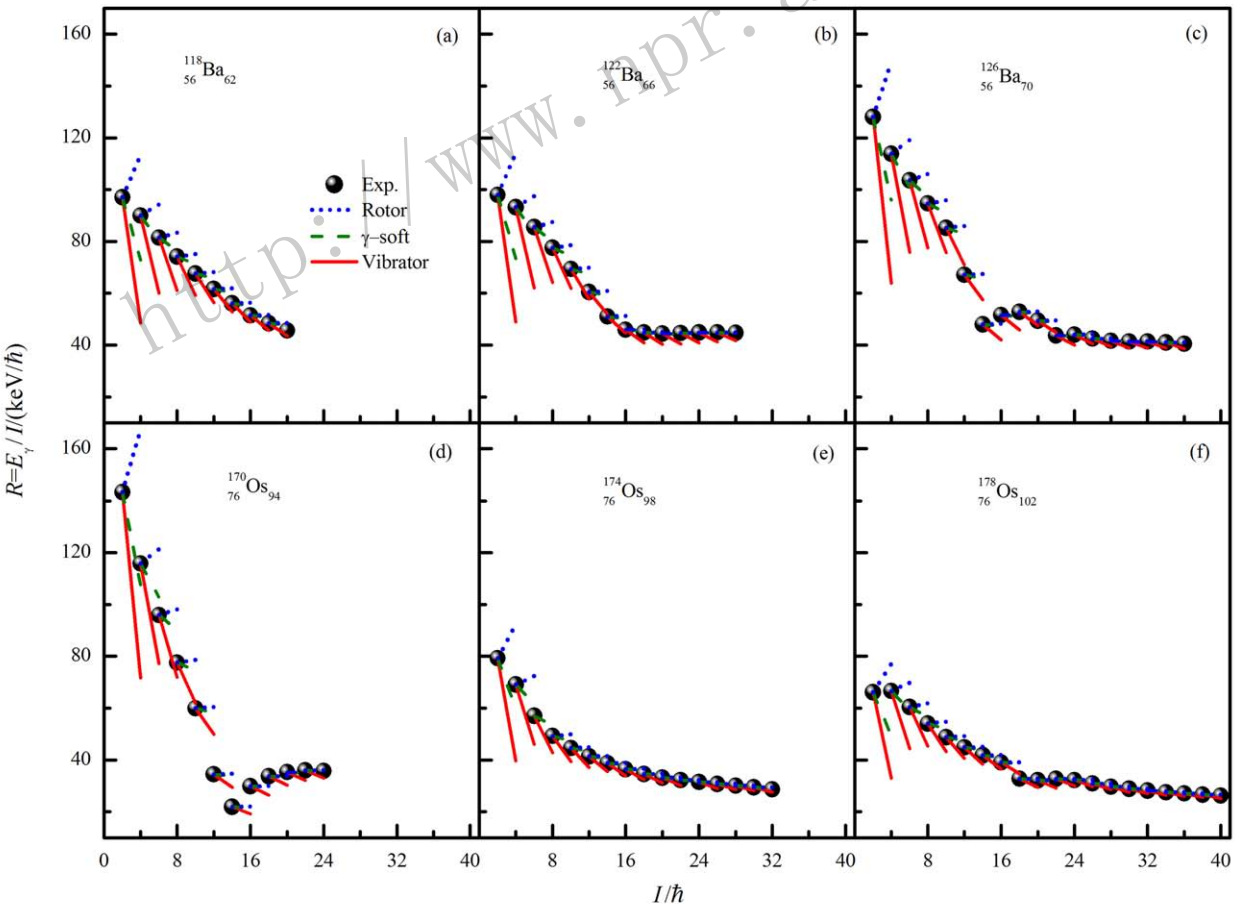

Fig. 6　(color online) The centipede-like E-GOS curves along the yrast lines for several selected Ba and Os nuclei.

4 Conclusions

In conclusion, nuclear shape and stiffness evolutions for even-even nuclei in $50 < Z < 82$ region are systematically investigated by using the NES calculation in the $(\beta_2, \gamma, \beta_4)$ deformation space. Our calculated results are compared with previous calculations and available data. It is found that the well-deformed nuclei have the relatively large stiffness parameters C_β and C_γ, while in the transition or near-spherical region, the nucleus will be soft, are in agreement with experiments. In the rotational cases, it seems that the vibration effect should not be ignored, especially in the transition nuclei. In addition, the nuclear stiffness in a deformation degree of freedom (*e.g.*, γ) depends on the distance to the corresponding magic number (*e.g.*, γ magic number) to a large extent rather than the mass regions(*e.g.*, light or heavy mass regions).

References:

[1] BOHR A, MOTTELSON B R. Nuclear Structure[M]. Singapore: World Scientific Publishing, 1998.
[2] FRAUENDORF S. Rev Mod Phys, 2001, **73**: 463.
[3] YANG Q, WANG H L, LIU M L, *et al.* Phys Rev C, 2016, **94**: 024310.
[4] YANG J, WANG H L, LIU M L, *et al.* Prog Theor Exp Phys, 2016, 063D03.
[5] WANG H L, YANG J, LIU M L, *et al.* Phys Rev C, 2015, **92**: 024303.
[6] WANG H L, ZHANG S, LIU M L, *et al.* Prog Theor Exp Phys, 2015, 073D03.
[7] CHAI Q Z, WANG H L, YANG Q, *et al.* Chin Phys C, 2015, **39**: 024101.
[8] YANG Q, WANG H L, CHAI Q Z, *et al.* Chin Phys C, 2015, **39**: 094102.
[9] WANG H L, LIU H L, XU F R, *et al.* Prog Theor Phys, 2012, **128**: 363.
[10] XU F R, WALKER P M, SHEIKH J A, *et al.* Phys Lett B, 1998, **435**: 257.
[11] NAZAREWICZ W, LEANDER G A, DUDEK J. Nucl Phys A, 1987, **467**: 437.
[12] SATUŁA W, WYSS R, MAGIERSKI P. Nucl Phys A, 1994, **578**: 45.
[13] MÖLLER P, NIX J R. Nucl Phys A, 1981, **361**: 117.
[14] MYERS W D, SWIATECKI W J. Nucl Phys A, 1966, **81**: 1.
[15] NAZAREWICZ W, RILLEY M A, GARRETT J D. Nucl Phys A, 1990, **512**: 61.
[16] STRUTINSKY V M. Nucl Phys A, 1967, **95**: 420.
[17] NAZAREWICZ W, DUDEK J, BENGTSSON R, *et al.* Nucl Phys A, 1985, **435**: 397.
[18] CWIOK S, DUDEK J, NAZAREWICZ W, *et al.* Comp Phys Comm, 1987, **46**: 379.
[19] PRADHAN H C, NOGAMI Y, LAW J. Nucl Phys A, 1973, **201**: 357.
[20] BHAGWAT A, VIÑAS X, CENTELLES M, *et al.* Phys Rev C, 2010, **81**: 044321.
[21] SATUŁA W, WYSS R. Rep Prog Phys, 2005, **68**: 131, and references cited therein.
[22] CASTEN R F, BRENNER D S, HAUSTEIN P E. Phys Rev Lett, 1987, **58**: 658.
[23] FOULADI N, FOULADI J, SABRI H. Eur Phys J Plus, 2015, **130**: 112.
[24] CASTEN R F. Phys Rev Lett, 1985, **54**: 1991.
[25] CASTEN R F. Nucl Phys A, 1985, **443**: 1.
[26] CASTEN R F, ZAMFIR N V. J Phys G: Nucl Part Phys, 1996, **22**: 1521.
[27] MALLMANN C A. Phys Rev Lett, 1959, **2**: 507.
[28] GUPTA J B. Int J Mod Phys E, 2013, **22**: 1350023.
[29] IACHELLO F. Phys Rev Lett, 2001, **87**: 052502.
[30] MÖLLER P, NIX J R, MYERS W D, *et al.* At Data Nucl Data Tables, 1995, **59**: 185.
[31] RAMAN S, NESTOR C W, TIKKANEN P, *et al.* At Data Nucl Data Tables, 2001, **78**: 1.
[32] DUDEK J, NAZAREWICZ W, OLANDERS P. Nucl Phys A, 1984, **420**: 285.
[33] ANDERSSON G, LARSSON S E, LEANDER G, *et al.* Nucl Phys A, 1976, **268**: 205.
[34] NAZAREWICZ W, OLANDERS P, RAGNARSSON I, *et al.* Nucl Phys A, 1984, **429**: 269.
[35] BUTLER P A, NAZAREWICZ W. Rev Mod Phys, 1996, **68**: 349.
[36] REGAN P H, BEAUSANG C W, ZAMFIR N V, *et al.* Phys Rev Lett, 2003, **90**: 152502.
[37] XU F R, WYSS R, WALKER P M. Phys Rev C, 1999, **60**: 051301.
[38] KIBÉDI T, DRACOULIS, BYRNE A P, DAVIDSON P M. Nucl Phys A, 2001, **688**: 669.
[39] KIBÉDI T, DRACOULIS G D, BYRNE A P, *et al.* Nucl Phys A, 1994, **567**: 183.
[40] DAVIDSON P M, DRACOULIS G D, KIBÉDI T. Nucl Phys A, 1999, **657**: 219.

http://www.npr.ac.cn

可能的原子核形状及硬度演化性质：基于能量面计算的系统分析

孟海燕[1]，王华磊[1,†]，柴清祯[1]，张 莎[1]，杨 婕[1]，柳敏良[2]

（1. 郑州大学物理工程学院，郑州 450001；
2. 中国科学院近代物理研究所，兰州 730000）

摘要： 基于 (β_2,γ,β_4) 形变空间下对-形变自洽的原子核能量面计算方法，系统研究分析了 $50<Z<82$ 区偶偶核的形状及硬度演化特征。计算的平衡形变与其它理论预言及存在的实验值进行了对比。从相应的形变势能曲线提取了与 β_2 及 γ 相关的硬度参数 C_β, C_γ，这与实验观测到的低位 β 及 γ 振动带信息相符。还简要讨论了转动情况下的硬度演化，例如基于蜈蚣型 E-GOS 曲线，表明存在不可忽略的振动效应。

关键词： 核形状；硬度参数；核能量面计算

http://www.npr.ac.cn

收稿日期： 2016-10-30；　**修改日期：** 2017-04-19

基金项目： 国家自然科学基金资助项目(11675148)；郑州大学优秀青年教师发展基金(1521317002)；郑州大学物理学科推进计划项目(32410017)；河南省基础与前沿技术研究计划项目(162300410222)

† **通信作者：** 王华磊, E-mail: wanghualei@zzu.edu.cn。